ACS APPLIED MATERIALS & INTERFACES

www.acsami.org

Research Article

High-Conductivity and High-Capacitance Electrospun Fibers for Supercapacitor Applications

Somdatta Bhattacharya, Indroneil Roy, Aaron Tice, Caitlyn Chapman, Ranodhi Udangawa, Vidhya Chakrapani, Joel L. Plawsky,* and Robert J. Linhardt*

Cite This: *ACS Appl. Mater. Interfaces* 2020, 12, 19369–19376

Read Online

ACCESS | Metrics & More | Article Recommendations | Supporting Information

ABSTRACT: Electrospinning is a simple method for producing nanoscale or microscale fibers from a wide variety of materials. Intrinsically conductive polymers (ICPs), such as polyaniline (PANI), show higher conductivities with the use of secondary dopants like *m*-cresol. However, due to the low volatility of most secondary dopants, it has not been possible to electrospin secondary doped ICP fibers. In this work, the concept of secondary doping has been applied for the first time to electrospun fibers. Using a novel design for rotating drum electrospinning, fibers were efficiently and reliably produced from a mixture of low- and high-volatility solvents. The conductivity of electrospun PANI–poly(ethylene oxide) (PEO) fibers prepared was 1.73 S/cm, two orders of magnitude higher than the average value reported in the literature. These conductive fibers were tested as electrodes for supercapacitors and were shown to have a specific capacitance as high as 3121 F/g at 0.1 A/g, the highest value reported, thus far, for PANI–PEO electrospun fibers.

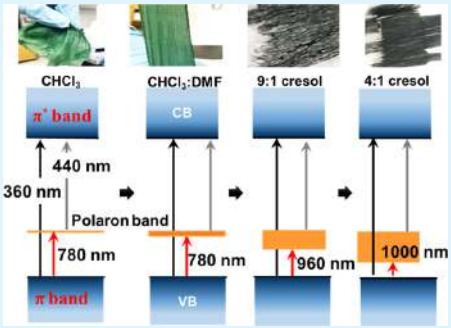

KEYWORDS: *electrospinning, polyaniline, conductive, cresol, dopants, high-boiling-point solvents, supercapacitors*

INTRODUCTION

Electrochemical energy-storage devices, particularly supercapacitors, have become increasingly popular in applications requiring high power densities.[1−3] The increased demand for eco-friendly and high-energy-density storage devices in electric vehicles and electronic circuits has made it crucial to find sustainable, lightweight, and flexible polymers for such applications. Polyaniline (PANI) is one of the oldest, intrinsically conducting polymers (ICPs), and its high stability, ease of synthesis, low monomer cost, and ease of altering its conductivity via doping make it one of the most well-studied conductive polymers.[4−6] PANI nanofibers have been used in a wide array of applications, including wearable electronics,[7] sensors,[8] actuators,[9] electrochromic glass displays,[10] electromagnetic shielding devices,[11] and supercapacitors.[12]

PANI nanostructures and nanocomposites have shown promising electrochemical performance by altering the nature of dopants used to make them conductive.[13−15] Such PANI-based nanocomposites are typically produced by using either simple bulk polymerization routes[16] or templated self-assembly.[17,18] All of these synthesis routes involve multiple steps and yield materials with low surface areas.[13,19] Due to these drawbacks, electrospun PANI fibers have received significantly greater attention compared to conventional bulk PANI or film-cast PANI.[20−22] In particular, the high surface area to volume ratio, short diffusion paths for dopant ions, and the relative ease of electrode fabrication make electrospun fibers a promising electrode material for supercapacitor applications.

The theoretical specific capacitance of PANI in sulfuric acid has been estimated to be 2000 F/g.[23] This high value has been difficult to achieve in practice because of limited charge-transfer rates, low conductivities, and incomplete doping levels.[24] Nevertheless, PANI capacitance values ranging from less than 500 F/g to over 3400 F/g have been reported.[19,25,26] However, because of variation in electrode components, device configuration, and methods of capacitance calculation, it is difficult to reliably compare the reported capacitance of PANI with theoretical capacitance.[24,27] Wang et al. have shown that the capacitance of PANI is highly dependent on the coating thickness, porosity of the PANI material, charging rate, and conductivity of PANI structures.[24]

Like other conducting polymers, PANI has a semirigid backbone owing to its high aromaticity and is available only in relatively low molecular weight. This creates a substantial obstacle for electrospinning as the elasticity of these solutions is generally insufficient to be spun into fibers. Several

Received: November 29, 2019
Accepted: April 10, 2020
Published: April 10, 2020

https://dx.doi.org/10.1021/acsami.9b21696
ACS Appl. Mater. Interfaces 2020, 12, 19369–19376

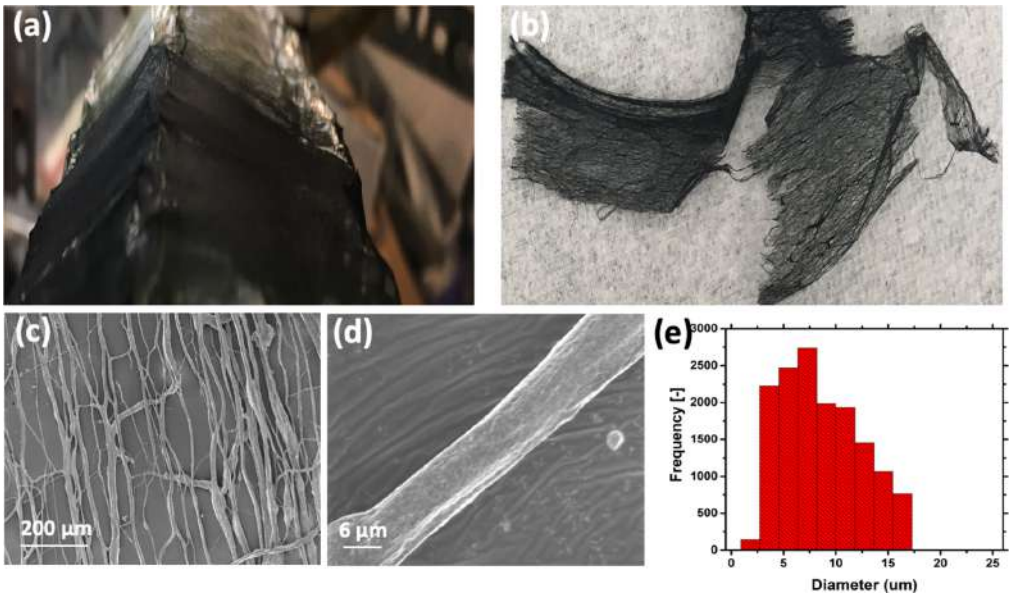

Figure 1. Electrospun freestanding conductive blended PANI−PEO fiber mats with the CSA dopant. (a) PANI−PEO fiber mat collected on a mandrel. (b) Aligned PANI−PEO fiber mat spun from *m*-cresol. (C) Scanning electron microscopy (SEM) imaging of the as-spun fiber mat (spun from 4:1 v/v chloroform/*m*-cresol). (d) Detailed view of a spun fiber (high magnification). (e) Plot showing the frequency of fiber diameter distribution.

approaches have been developed to circumvent this challenge. One of these approaches is to use concentrated sulfuric acid, which is a highly corrosive solvent, for wet−wet electrospinning of pure PANI nanofibers.[28] This method has not gained much attention because of its difficulty in processing the fibers, as well as the safety risks associated with electrospinning from a corrosive solvent. Another strategy is to blend PANI with other high-molecular-weight carrier polymers like poly(methyl methacrylate) (PMMA),[29] polycaprolactone (PCL),[30] and poly(ethylene oxide) (PEO).[31] Carrier polymers like PEO are necessary to increase the viscosity of the solution and enhance the ability to spin fibers. PEO itself provides no improvement to the conductivity and specific capacitance of the composite fibers and may even reduce the performance of the fibers because it is an insulating material. These reports demonstrate the formation of the nanofibers, but the electrical properties of these fibers have not been reported. The average electrical conductivity reported for such PANI fiber blends, using a four-probe conductivity measurement, is of the order of 10^{-2} S/cm.[32,33] Lee et al.[31] reported a conductivity of 33 S/cm for the PANI−PEO-blended fibers, where the PEO content was 50% of the total composition. However, in this work, the PANI−PEO fibers were not aligned. They also could not be easily isolated from the collector, making these fibers difficult to use in various applications. The highest conductivity (50 ± 30 S/cm) of unstretched pure PANI nanofibers (after removal of the carrier polymer) was reported by Rutledge et al.,[34] where the conductivity was measured using interdigitated Pt electrodes. These nanofibers were synthesized using a two-step process, with the second step involving removal of the carrier polymer.

In this article, we report an approach to electrospin aligned, conductive blended PANI−PEO microfibers with camphorsulfonic acid (CSA) as a primary dopant in a single step from a mixture of low- and high-volatility solvents (*m*-cresol and chloroform) that overcomes these challenges. The resulting fibers show an electrical conductivity of 1.73 S/cm that is substantially higher than the average values reported for PANI−PEO fibers. Our approach involves the fabrication of a mesh mat comprised of freestanding, well-aligned conductive fibers having multiple branches to facilitate electron conduction (Figure 1). This fiber mat was fabricated using a secondary dopant, *m*-cresol. We also report the effect of different solvents/dopants on PANI−PEO fiber conductivity. Finally, this fiber mesh was used as a thin, stand-alone, flexible electrode in an electrochemical supercapacitor showing a very high specific capacitance.

EXPERIMENTAL SECTION

Chemicals. Polyaniline (PANI, emeraldine base, M_w = 65 000) and poly(ethylene oxide) (PEO, M_w = 2 000 000 g/mol), (+)-camphor-10-sulfonic acid (CSA), *m*-cresol, and chloroform (high-performance liquid chromatography (HPLC) grade) were purchased from Sigma-Aldrich, St. Louis, MO. All materials were used without further purification.

Sample Preparation. CSA (0.087 g, 0.37 mmol) was dissolved in a 10 mL mixture of chloroform and *m*-cresol with volume ratios of 9:1 and 4:1. PANI (0.068 g, 1.05 μmol) was added to the solution slowly and was kept under magnetic stirring at 25 °C for 24 h. The solution was then filtered using a 0.45 μm Nylon filter (25 mm in diameter). PEO (0.085 g, 40 nmol) was then dissolved in these solutions and was kept under magnetic stirring overnight.

Electrospinning. The potential difference for electrospinning was generated using a high-voltage supplier (ES 50P-5W, γ High Voltage Research Inc.) and was kept at or below +25 kV. This is below (usually ∼40−50 kV) the voltage requirements for low volatility solvents (i.e., dimethylformamide (DMF)) previously reported.[34] A monoaxial spinneret (MECC, Ogori, Fukuoka, Japan) was fitted with a blunt-tip aluminum needle (23 gauge) that has an outer diameter of 0.64 mm. The needle tip-to-collector surface distance was varied between 20 and 26 cm. Highly aligned fibers were formed perpendicular to the orientation of the aluminum rods. The flow

https://dx.doi.org/10.1021/acsami.9b21696
ACS Appl. Mater. Interfaces 2020, 12, 19369−19376

rate of the solutions was controlled by a syringe pump (NE-1000, New Era Pump System Inc., Wantagh, New York) and varied from 1 to 1.5 mL/h. The temperature and humidity in the electrospinning box were constantly monitored using a digital humidity and temperature monitor (AcuRite) and was maintained at 20 ± 3 °C and 16%, respectively.

Fiber Characterization. *Thermogravimetric Analysis (TGA).* The PANI−PEO microfibers, pure PANI, pure CSA, and pure PEO were analyzed on a computer-controlled TGA-Q50 apparatus (New Castle, Delaware). The samples were heated from room temperature to 1000 °C at a constant heating rate of 1 °C/min under constant nitrogen flow. The average decomposition temperatures and the shift in decomposition peaks were determined by TA Instruments Universal Analysis software V4.7A. Furthermore, TA Instruments defines the detection limit of TGA to 0.1% by mass of the sample.

Morphology Composition. A Carl Zeiss Supra field emission scanning electron microscope (Hillsboro—resolution at 1 kV—2.5 nm) was used to investigate the morphology of the different fibers. The average fiber diameters were calculated using NIH ImageJ software (National Institute of Health, MD). Diameters from around 3000 individual fibers from 10 identical electrospinning experiments were employed in this fiber diameter analysis.

Crystalline Structure. The crystallinity of 4:1 and 9:1 fibers was studied using a Bruker D8-DISCOVER X-ray diffractometer and compared with that of pure PANI powder. The X-ray diffraction (XRD) pattern analysis was performed using Bruker's DIFFRAC.EVA software.

Optical Absorption Spectroscopy. All optical absorbance measurements of the fiber samples were recorded using an ultraviolet (UV)−vis−near-infrared (NIR) spectrophotometer (Shimadzu UV-3600) in the range of 300−2600 nm. Absorption spectra of PANI−PEO fibers prepared using different solvents were recorded in the diffuse reflectance mode by dispersing a known amount of the fiber sample onto a $BaSO_4$ pellet.

Four-Probe Conductivity Measurement. The current−voltage characteristic was measured using a digital electrometer and stabilized power supply. The method usually uses a linear array of four equally spaced tips that are pressed onto the surface of the material. A voltage sweep from −0.005 to +0.005 V was carried out through the two outer probes and the current was measured across the two inner probes. The resistivity is measured by eq 1

$$\rho = (V/I)^*A/t \quad (1)$$

where ρ is the resistivity, V is the voltage measured, I is the current passed, t is the thickness of the fiber mat, which was measured using a profilometer (Bruker Optical Profilometer), and A is the area of the fiber mat (distance between two probes multiplied by the width of the mat). The conductivity of the mat was calculated by eq 2

$$\sigma = 1/\rho \quad (2)$$

where σ is the conductivity.

Electrochemical and Spectroelectrochemical Testing. *Supercapacitor Testing.* Cyclic voltammetry and galvanostatic charge/discharge testing were performed on a standard three-electrode device with the PANI−PEO fibers as the working electrode, saturated calomel (SCE) electrode as the reference electrode, and a platinum wire as the working electrode at room temperature in an air-saturated 1 M H_2SO_4 electrolyte. The PANI−PEO electrode was fabricated using a poly(tetrafluoroethylene) (PTFE) connector (Swagelok), a 1/4″ graphite rod, and as-prepared PANI−PEO fiber mat of known mass. No conducting carbon or binders were used. The fiber mat was held down on the PTFE connector and kept in place by the pressure applied by a conducting graphite rod. A picture of the electrode device is shown in Supporting Information (SI), Figure S3. All testing was performed using a CHInstruments 660E potentiostat.

The specific capacitance of the fiber electrodes was calculated from the cyclic voltammetry (CV) curves according to eq 3

$$C = \frac{Q}{\Delta V^*m} \quad (3)$$

where C (F/g) is the specific capacitance, $Q(C)$ is the average charge during the charging and discharging process, m(g) is the mass of the active materials on the working electrode, and $\Delta V(V)$ is the potential window.

In situ Spectroelectrochemical Testing. In situ UV/VIS measurements were carried out on PANI−PEO electrodes in the transmission mode during electrochemical cycling in 1 M H_2SO_4 to detect the redox changes to understand the origin of the capacitive behavior of PANI−PEO fibers. Electrodes used for these measurements were prepared by dispersing a known weight of the fiber in isopropyl alcohol, which was then sonicated and drop-cast on a conductive fluorine-doped tin oxide (FTO)-coated glass slide. This process resulted in a semitransparent continuous film that was suitable for transmission measurements. Measurements were performed in a cuvette in 1 M H_2SO_4 with a three-electrode device using the PANI−PEO/FTO slide as the working electrode, a silver foil as the reference electrode, and a Pt wire as the counter electrode. The potential of the Ag foil reference electrode was calibrated with a ferri−ferrocyanide redox couple using a Pt disc working electrode. All reported potentials are with respect to the potential of the SCE/saturated KCl electrode, which has a reference potential of 0.197 V versus the standard hydrogen electrode (SHE). The absorbance spectrum of the electrode was recorded after the application of a step voltage for 10 min at different positive and negative voltages in the range of −0.4 to +1 V.

RESULTS AND DISCUSSION

To make PANI solutions highly conductive, one of the popular approaches is the use of secondary dopants, like *m*-cresol, *p*-cresol, *o*-chlorophenol, and *m*-ethylphenol,[35] which increases the crystallinity and conductivity of the polymer.[36] PANI ES is a polyelectrolyte in which the polymer chain is positively charged and negative counter ions of the primary dopant are in close proximity. In the presence of these solvents, the PANI emeraldine salt polyelectrolyte forms a network of H-bonds with the phenol groups of the secondary dopants. This provides an effective proton-exchange medium in which the negative charges of the primary dopants are removed. Owing to a static repulsive interaction, the positive charges on the polymer backbone tend to spread over the polymer chain, forming an extended polymer structure.[37] Thus, a PANI with a primary dopant, like camphorsulfonic acid (CSA), in a secondary dopant, like *m*-cresol, can afford conductivities as high as 300 S/cm[38] in its solution state.

Four different solution sets were selected (Table S1) to understand the role of solvents in increasing CSA-doped PANI−PEO fiber conductivity. Fibers were easily formed by electrospinning from chloroform and a mixture of chloroform and DMF. However, forming fibers from a mixture of chloroform and *m*-cresol was considerably more challenging. One parameter that plays an important role in the process of electrospinning PANI−PEO fibers is solvent volatility. Since *m*-cresol is a liquid at room temperature and has a high boiling point, a mixture of highly volatile chloroform with low-volatility *m*-cresol was examined to promote evaporation in the electrospinning process. Unfortunately, in the electrospinning process, the chloroform evaporates first, leaving liquid *m*-cresol behind, which then only slowly evaporates, resulting in wet fibers that can fuse. We separate the collection points from the body of the rotating drum to allow more of the low-volatile solvent to evaporate. This was done by including a series of metal rods that were attached parallel to the drum surface. Fibers were then collected on the rods, allowing for air flow through the entire mat and adequate drying of the deposited fibers. The resulting fibers could then be easily and completely recovered intact from the aluminum rods on the rotary drum

https://dx.doi.org/10.1021/acsami.9b21696
ACS Appl. Mater. Interfaces 2020, 12, 19369−19376

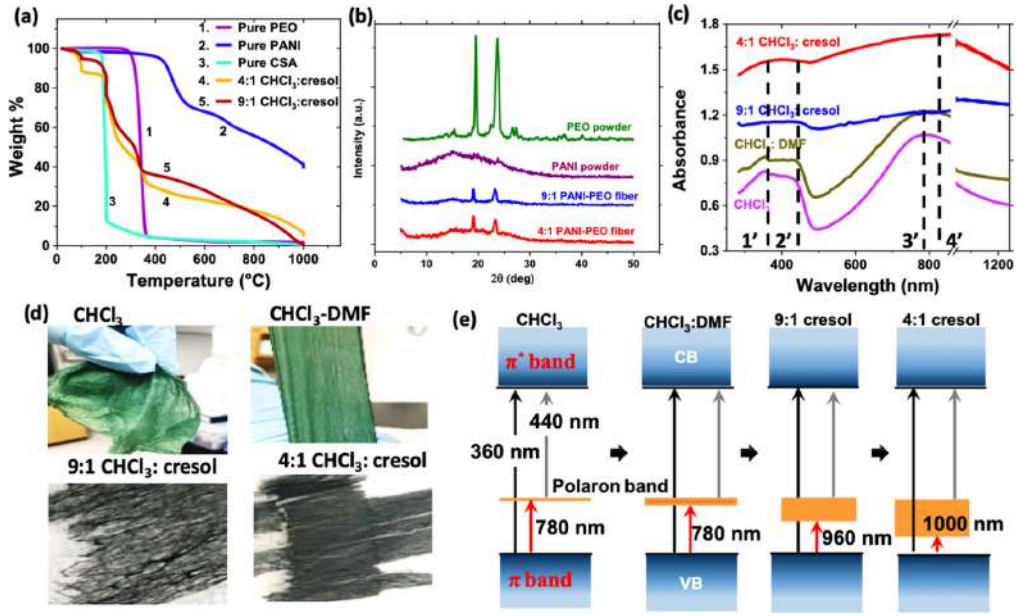

Figure 2. Characterization of blended PANI–PEO fibers and PANI energy band diagrams. (a–d) Characterization of blended fiber samples—(a) TGA of 9:1 and 4:1 PANI–PEO fibers and their individual components showing decomposition peaks. (b) XRD of pure PANI powder showing an amorphous peak for the 4:1 and 9:1 blended fibers, confirming the crystalline nature of the as-prepared fibers. (c) Optical absorption spectrum of the four different fiber sets, indicating changes in the electronic properties of the different fiber sets. (d) Images of the spun fiber mats. (e) Schematic of the energy band diagram of PAN–PEO spun using various solvents. Also shown are the various electronic transitions in these materials observed in the optical absorption measurements.

collector. The resulting fiber mats were lyophilized overnight to obtain dry fiber mats for testing. While a majority of previous studies on PANI–PEO fibers involved electrospinning from chloroform and chloroform:DMF mixtures, the current study focused on the characterization of the properties of PANI–PEO fibers electrospun from solvent mixtures containing *m*-cresol, a secondary dopant.

TGA of PANI–PEO-blended fibers electrospun from solvent mixtures containing *m*-cresol was used to characterize the chemical and physical properties of the electrospun fibers. The thermograms (Figure 2a) show shifts in the CSA primary dopant and PEO carrier peaks in both 9:1 and 4:1 microfibers. The weight derivative thermograms also showed that the degradation curves of the blended PANI–PEO fibers indicate the integrated thermal behaviors of PEO, PANI, and CSA.

These structural changes were further corroborated using X-ray diffraction (XRD) analysis.[39] XRD was employed to monitor the structural changes that occur in the PANI–PEO-blended microfibers compared to pure PANI and PEO powder. The PEO powder has two sharp crystalline peaks at 2θ = ~19.5 and ~24.5°, which suggests a semicrystalline nature. The sharp peaks observed at 2θ = ~19 and ~24° in the PANI–PEO fibers (Figure 2b) are ascribed to the periodicity parallel and perpendicular to the PANI chains, respectively.[13,19,40,41] The presence of these peaks indicates a degree of crystallinity within the microfibers that might have been induced due to the presence of primary and secondary dopants, as well as extensional forces during electrospinning.[19,36] However, these peaks could also be a contribution from PEO. The pure PANI powder showed a broad amorphous peak, further suggesting that the molecular arrangement of the PANI polymer in blended microfibers is more ordered in the parallel and perpendicular directions and that the polymer backbone chain is oriented along the fiber axis.[42] Differential scanning calorimetry (DSC) was also carried out to measure the glass transition temperatures of these blended fibers (Figure S2). Optical absorption measurements in the ultraviolet (UV) to near-infrared (NIR) spectral range were performed in the diffuse reflectance mode by dispersing a known amount of the fiber sample onto a $BaSO_4$ pellet and are shown in Figure 2c. Blended fibers that were spun from solvents such as chloroform and DMF showed three sharp peaks at 360 (represented by 1′ in Figure 2c), 440 (represented by 2′ in Figure 2c), and 780 nm (represented by 3′ in Figure 2c). These wavelengths have previously been attributed to the three electronic transitions (Figure 2e): π–π^* band transition, polaron band to π^* band, and π band to polaron band transitions, respectively. While these transitions are also observable in 9:1 and 4:1 fiber samples, the spectrum of these samples is dominated by the polaron (defect)-related peak, namely, the π band to polaron peak, in the infrared spectral range. The high absorbance value of this peak together with the observed red shift from ~780 to ~1100 nm (represented by 4′ in Figure 2c) is indicative of the formation of a broader (or dispersive) polaron band in the blended fibers spun with *m*-cresol than those spun from chloroform or DMF, and therefore they may be highly conductive. This is shown schematically in Figure 2e. This observation corroborates the previous results on thin PANI films.[36,43] Figure 2d shows the as-spun fiber mats prepared from the four starting solutions. PANI–PEO fibers spun out of chloroform and DMF have a lighter color than *m*-cresol because in the presence of *m*-cresol the PANI chains become more extended and hence show an

https://dx.doi.org/10.1021/acsami.9b21696
ACS Appl. Mater. Interfaces 2020, 12, 19369–19376

increased conductivity, corroborating the previously published literature.[35,37,39]

The electrical conductivity of aligned, electrospun-blended fibers was confirmed using a four-probe conductivity measurement in Van der Pauw geometry. The conductivities for 9:1 and 4:1 samples were 1.34 ± 0.333 and 1.73 ± 0.28 S/cm, respectively (Table 1). The blended microfibers spun from *m*-cresol show at least two orders of magnitude higher conductivities than fibers spun without this secondary dopant.

Table 1. Conductivity of PANI−PEO-Blended Nanofibers Spun from Various Solvents

solvent used in electrospinning	conductivity (S/cm)	diameter of the fibers (nm)
chloroform: *m*-cresol (4:1)	1.73 ± 0.28	8000
chloroform: *m*-cresol (9:1)	1.34 ± 0.33	3500
chloroform: DMF	8.5×10^{-3}	653
chloroform	1.5×10^{-8}	525

The high electrical conductivity values for the PANI−PEO-blended nanofibers spun from solvents containing CSA and *m*-cresol as primary and secondary dopants, respectively, motivated us to examine these spun fiber mats as electrodes in supercapacitors.

Our electrospun PANI−PEO fiber mats represent a unique alternative to traditional methods for making electrodes because of the ease in which these mats can be fabricated. Electrodes for supercapacitors are typically prepared by mixing the PANI nanostructures with binders such as poly(tetrafluoroethylene) (PTFE) and other conductive additives like porous activated carbon powder.[44,45] This traditional method requires a processing time of ∼2−12 h and involves many fabrication steps. In contrast, electrospun PANI−PEO fiber mat electrodes can be prepared in minutes in a single step. Both pure PANI and PANI-based composites have previously been used in supercapacitor applications and are highlighted in a review article by Eftekhari et al.[2] The highest capacitance reported, thus far, for an electrode based on pure PANI nanofibers is 636 F/g.[46] Additionally, in most of these previously reported cases, the nanofibers were not free-standing. Most PANI−PEO fibers have been tested using a conventional approach to prepare supercapacitor electrodes with powdered nanofibers and insulating binders.[47,48] Simotwo et al.[19] developed supercapacitor electrodes using freestanding PANI/PEO and PANI/CNT/PEO fiber mats prepared by electrospinning. An electrochemical supercapacitor based on these fibers showed specific capacitances of 308 and 385 F/g. To our knowledge, this is the only study that has reported the capacitance of electrospun PANI−PEO fibers. The addition of a relatively high fraction of a chemically inert and insulating carrier polymer and the eesential addition of carbon nanotubes to improve the specific capacitance make these no longer purely polymer-based nanofiber electrodes and also require a complex fabrication process.

The pseudocapacitive performance of our freestanding electrospun PANI−PEO fiber mat electrodes was investigated using cyclic voltammetry (CV) at room temperature with a voltage window of −0.2−0.8 V and scan rates from 5 to 100 mV/s (Figure 3a). The potential intervals of galvanostatic charge/discharge (GCD) tests were chosen to be consistent with prior literature reports on PANI (Table S3). We looked for gas evolution reactions at either side of the potential window. Since gas evolution shows the breakdown of aqueous electrolytes, we can determine the range in which we can run the CV. Both 9:1 and 4:1 fibers exhibit well-defined, reversible pairs of redox peaks in the voltage range of 0.1−0.3 V versus an SCE reference electrode. Similar peaks in the same voltage range were observed previously in thin-film electrodes, and the first peak has been attributed to redox transitions between the

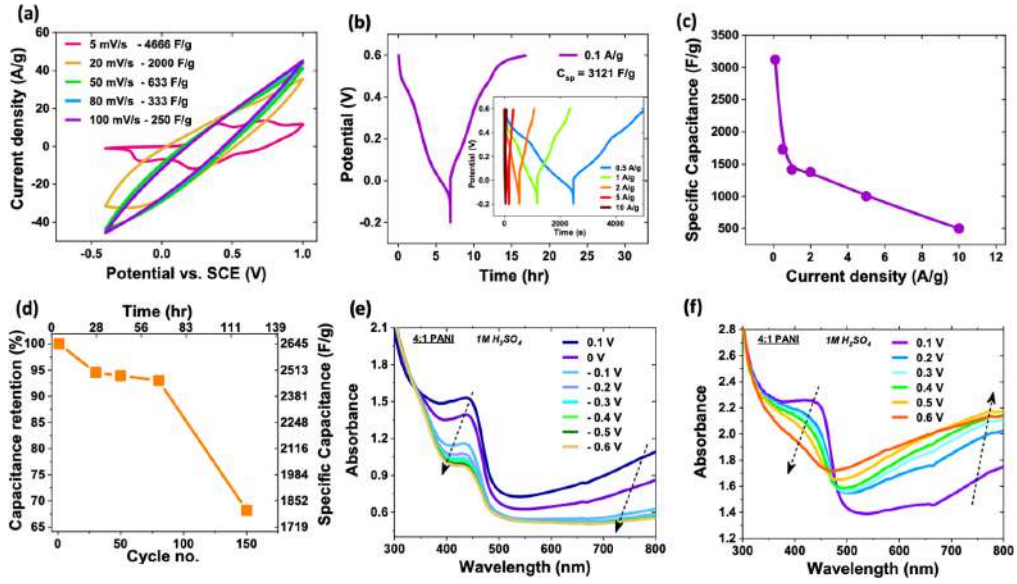

Figure 3. Electrode testing for supercapacitor applications. (a) Cyclic voltammetry at different scan rates for 4:1 blended fibers. (b) Cyclic charge−discharge curves of 4:1 blended fibers at different current densities. (c) Specific capacitance as a function of different scanning rates from cycles. (d) Results of long-term galvanostatic testing at the rate of 1 A/g showing a drop in specific capacitance over 80 cycles. (e and f) In situ UV−vis experiments showing change in the absorbance of PANI−PEO fibers during positive (e) and negative (f) polarization in 1 M H_2SO_4.

https://dx.doi.org/10.1021/acsami.9b21696
ACS Appl. Mater. Interfaces 2020, 12, 19369−19376

leucoemeraldine and emeraldine states, while the second pair of peaks corresponded to the emeraldine−pernigraniline redox transitions.[19] The capacitance of our blended PANI−PEO fiber mat electrode, calculated from the CV curve at 5 mV/s (see the Experimental Section), showed a specific capacitance of 4666 F/g, almost 16 times higher than that previously reported for a pure PANI electrode under similar test conditions. However, no significant redox peaks were observed at higher scan rates. Several factors may contribute to the loss (or shift) of the redox peaks at higher scan rates. At higher scan rates, there are kinetic and mass transfer limitations associated with intercalating dopant ions throughout the PANI fiber structure. At these higher scan rates, ions accumulate only on the outer surface due to lower residence time and, hence, the redox reactions cannot be carried out effectively. At lower scan rates, these limitations are relaxed, and electrolyte/dopant ions have sufficient time to penetrate the pores of the material and hence change the redox states. Kinetic limitations shift the anodic peak potential to more positive voltages at a higher scan rate. Based on the previously published literature,[49−52] the loss of peaks suggests a specific transition that makes either the redox peaks in the CV thermodynamically unstable or the kinetics of the redox reactions much slower than the scan rates. During the oxidation−reduction process of polyaniline, protons get exchanged from the electrolyte and electrode interface. At higher scan rates, the proton transfer process is slow. This leads to either depletion or saturation of the protons during the redox process, which limits the redox reactions and, hence, the loss of peaks. The electrodes were also tested galvanostatically at various charge−discharge rates using current densities in the range of 0.1−10 A/g and a potential scan window of 0.8 V (−0.2−0.6 V), as shown in Figure 3b,c. The maximum specific capacitance value of 3121 F/g was obtained at 0.1 A/g (Figure 3c) under galvanostatic testing. The capacity reported in our work is higher than the theoretical capacitance of PANI calculated of 1255 F/g for a potential window of 0.8 V. This calculation of the theoretical capacitance is based on the assumption of one proton insertion into one aniline unit, to be consistent with the calculation method performed by Li et al.[23] Our results suggest that in highly conductive PANI, more than one proton may be able to intercalate into the aniline unit, thus resulting in capacities higher than the theoretical value. Reports of specific capacitances of 3407 F/g have been reported by other groups.[25]

At the highest rate tested, 10 A/g, the specific capacitance was 500 F/g, higher than that reported in previous studies of PANI electrodes (150 F/g).[19] The observed drop in capacitance increased with the increasing scan rate. This may be because at lower scan rates the electrolyte ions have sufficient time to penetrate the pores of the material, while at higher scan rates electrolyte ions accumulate on the outer surface. A long-term cycling test (Figure 3d) showed that fiber electrodes were stable even up to 325 700 s (~90 h) of continuous cycling, which corresponds to 80 charge−discharge cycles at 1 A/g. The value of specific capacitance decreased from the 2810 F/g observed at the beginning of the cycling to 2375 F/g at the end of 80 cycles, corresponding to almost 85% retention of specific capacitance. PANI has been shown to undergo volumetric changes during the protonation and deprotonation processes as a result of repeated insertion and deinsertion of ions, resulting in the deterioration of performance over the course of operations.[26] The results of XRD, SEM (Figure S4), and electrical conductivity measurements, performed on PANI−PEO fibers post electrochemical testing, showed a loss of crystallinity with cycling. However, the electrodes retained fiber morphology, and, while still showing an electrical conductivity of 0.001 S/cm, suggested some leaching of the secondary dopant *m*-cresol into the electrolyte during cycling. In our case, the leaching of secondary dopants is also a factor that leads to poor cycling stability. Additional studies are required to understand the mechanism of the loss of crystallinity and secondary dopant.

We assessed the optical absorbance of the PANI−PEO electrodes in situ during various stages of electrochemical polarization to understand the mechanism of charge storage in PANI (Figure 3e,f). The application of negative polarization (Figure 3e) leads to a strong reduction in the absorbance peak at 440 nm and along with a decrease in the NIR absorbance in the spectral range between 600 and 800 nm. Since the absorbance peak at 440 nm corresponds to the characteristic peak of the emeraldine (polaron) phase, the results indicate that increasing H^+ insertion at successive negative potentials leads to the increasing conversion of the emeraldine phase to the leucoemeraldine phase. Positive polarization (Figure 3f), leading to H^+ deinsertion, results in a decrease in the absorbance at potentials higher than 0.1 V. This trend is consistent with the initial oxidization of leucoemeraldine to the conducting emeraldine state of PANI followed by over-oxidation of the emeraldine phase to pernigraniline phase, a fully deprotonated form of PANI, at higher potentials.

CONCLUSIONS

In summary, we have engineered a method to electrospin polymers from high-boiling-point solvents at a relatively low voltage. Using this method, we have prepared electrospun fibers of PANI blended with PEO, with CSA as the primary dopant and *m*-cresol as the secondary dopant, providing an entirely new, one-step method to process highly aligned and highly branched electrospun fibers with high electrical conductivities. The conductivities of these fibers increased with the increase in the content of the secondary dopant, *m*-cresol. Conductivities as high as 1.73 S/cm were measured and these fibers exhibited a very high specific capacitance of up to 3121 F/g at 0.1 A/g when used as electrodes for supercapacitors under galvanostatic testing. The improved electrochemical performance of these fiber mat electrodes was facilitated by the combination of good inter- and intrafiber porosity, which promotes ion diffusion in the active sites, resulting in the high conductivity of these composites. Moreover, the freestanding nature of these electrodes (Figure S3) eliminates the need for complex processing and reduces the resources required for preparing electrodes for supercapacitors.

ASSOCIATED CONTENT

Supporting Information

The Supporting Information is available free of charge at https://pubs.acs.org/doi/10.1021/acsami.9b21696.

Electrospinning solutions; TGA analysis; DSC methods and curves; GC analysis of residual solvents; picture of the test electrode; XRD and SEM analyses of blended fibers after 80 cycles (PDF)

https://dx.doi.org/10.1021/acsami.9b21696
ACS Appl. Mater. Interfaces 2020, 12, 19369−19376

AUTHOR INFORMATION

Corresponding Authors

Joel L. Plawsky − *Howard P. Isermann Department of Chemical and Biological Engineering, Center for Biotechnology and Interdisciplinary Studies, Rensselaer Polytechnic Institute, Troy, New York 12180, United States*; Phone: (518) 276-6049; Email: plawsky@rpi.edu

Robert J. Linhardt − *Howard P. Isermann Department of Chemical and Biological Engineering, Center for Biotechnology and Interdisciplinary Studies and Department of Chemistry and Chemical Biology, Rensselaer Polytechnic Institute, Troy, New York 12180, United States*; orcid.org/0000-0003-2219-5833; Phone: (518) 276-3404; Email: linhar@rpi.edu

Authors

Somdatta Bhattacharya − *Howard P. Isermann Department of Chemical and Biological Engineering, Center for Biotechnology and Interdisciplinary Studies, Rensselaer Polytechnic Institute, Troy, New York 12180, United States*

Indroneil Roy − *Howard P. Isermann Department of Chemical and Biological Engineering, Center for Biotechnology and Interdisciplinary Studies, Rensselaer Polytechnic Institute, Troy, New York 12180, United States*

Aaron Tice − *Department of Mechanical, Aerospace and Nuclear Engineering, Rensselaer Polytechnic Institute, Troy, New York 12180-3590, United States*

Caitlyn Chapman − *Department of Chemistry and Chemical Biology, Rensselaer Polytechnic Institute, Troy, New York 12180-3590, United States*

Ranodhi Udangawa − *Department of Chemistry and Chemical Biology, Rensselaer Polytechnic Institute, Troy, New York 12180-3590, United States*; orcid.org/0000-0001-7482-7260

Vidhya Chakrapani − *Howard P. Isermann Department of Chemical and Biological Engineering, Center for Biotechnology and Interdisciplinary Studies, Rensselaer Polytechnic Institute, Troy, New York 12180, United States*; orcid.org/0000-0003-2682-3833

Complete contact information is available at: https://pubs.acs.org/10.1021/acsami.9b21696

Author Contributions

S.B. designed and performed the experiments, analyzed the data, and drafted the manuscript. I.R., A.T., C.C., and R.U. initiated and helped design the experiments. V.C., J.L.P., and R.J.L. helped designed the experiments and provided funding for this project and contributed to the writing and revision of the manuscript.

Notes

The authors declare no competing financial interest.

ACKNOWLEDGMENTS

This research was funded by grants from the National Institutes of Health DK111958 (R.J.L.), New York State SCRIB DOH01-PART2-2017 (R.J.L.), and NASA NNX13AQ78G. The authors acknowledge the following people for their assistance in handling the characterization instruments: Bryant C. Colwill, Sarah An, and David Frey from the Center for Integrated Electronics for Four-Probe Conductivity and SEM Assistance; CBIS analytical core facility director Dr. Joel Morgan for TGA and DSC assistance; Nick Smieszek for his assistance in in situ UV−vis experiments; and William F. Flaherty and Dr. Corey Woodcock for assistance in designing the rotating electrospinning mandrel.

REFERENCES

(1) Abrigo, M.; McArthur, S. L.; Kingshott, P. Electrospun Nanofibers as Dressings for Chronic Wound Care: Advances, Challenges, and Future Prospects. *Macromol. Biosci.* **2014**, *14*, 772−792.

(2) Eftekhari, A.; Li, L.; Yang, Y. Polyaniline Supercapacitors. *J. Power Sources* **2017**, *347*, 86−107.

(3) Karthikeyan, K.; Amaresh, S.; Lee, S.-N.; An, J.-Y.; Lee, Y.-S. High-Power Lithium-Ion Capacitor Using $LiMnBO_3$ -Nanobead Anode and Polyaniline-Nanofiber Cathode with Excellent Cycle Life. *ChemSusChem* **2014**, *7*, 2310−2316.

(4) Ding, X.; Han, D.; Wang, Z.; Xu, X.; Niu, L.; Zhang, Q. Micelle-Assisted Synthesis of Polyaniline/Magnetite Nanorods by in Situ Self-Assembly Process. *J. Colloid Interface Sci.* **2008**, *320*, 341−345.

(5) Kim, B. J.; Oh, S. G.; Han, M. G.; Im, S. S. Preparation of Polyaniline Nanoparticles in Micellar Solutions as Polymerization Medium. *Langmuir* **2000**, *16*, 5841−5845.

(6) Li, D.; Huang, J.; Kaner, R. B. Polyaniline Nanofibers: A Unique Polymer Nanostructure for Versatile Applications. *Acc. Chem. Res.* **2009**, *42*, 135−145.

(7) Tseng, R. J.; Huang, J.; Ouyang, J.; Kaner, R. B.; Yang, Y. Polyaniline Nanofiber/Gold Nanoparticle Nonvolatile Memory. *Nano Lett.* **2005**, *5*, 1077−1080.

(8) Sadek, A. Z.; Wlodarski, W.; Kalantar-Zadeh, K.; Baker, C.; Kaner, R. B. Doped and Dedoped Polyaniline Nanofiber Based Conductometric Hydrogen Gas Sensors. *Sens. Actuators, A* **2007**, *139*, 53−57.

(9) Gao, J.; Sansiñena, J.; Metals, H. W.-S. 2003, U. Chemical Vapor Driven Polyaniline Sensor/Actuators. *Synth. Met.* **2003**, *135−136*, 809−810.

(10) Erro, E. M.; Baruzzi, A. M.; Iglesias, R. A. Fast Electrochromic Response of Ultraporous Polyaniline Nanofibers. *Polymer* **2014**, *55*, 2440−2444.

(11) Wang, W.; Gumfekar, S. P.; Jiao, Q.; Zhao, B. Ferrite-Grafted Polyaniline Nanofibers as Electromagnetic Shielding Materials. *J. Mater. Chem. C* **2013**, *1*, 2851−2859.

(12) Jang, J.; Bae, J.; Choi, M.; Yoon, S. H. Fabrication and Characterization of Polyaniline Coated Carbon Nanofiber for Supercapacitor. *Carbon* **2005**, *43*, 2730−2736.

(13) Miao, Y. E.; Fan, W.; Chen, D.; Liu, T. High-Performance Supercapacitors Based on Hollow Polyaniline Nanofibers by Electrospinning. *ACS Appl. Mater. Interfaces* **2013**, *5*, 4423−4428.

(14) Xu, D.; Xu, Q.; Wang, K.; Chen, J.; Chen, Z. Fabrication of Free-Standing Hierarchical Carbon Nanofiber/Graphene Oxide/Polyaniline Films for Supercapacitors. *ACS Appl. Mater. Interfaces* **2014**, *6*, 200−209.

(15) Xu, J.; Wang, K.; Zu, S. Z.; Han, B. H.; Wei, Z. Hierarchical Nanocomposites of Polyaniline Nanowire Arrays on Graphene Oxide Sheets with Synergistic Effect for Energy Storage. *ACS Nano* **2010**, *4*, 5019−5026.

(16) Yan, Y.; Cheng, Q.; Wang, G.; Li, C. Growth of Polyaniline Nanowhiskers on Mesoporous Carbon for Supercapacitor Application. *J. Power Sources* **2011**, *196*, 7835−7840.

(17) Zhong, W.; Deng, J.; Yang, Y.; Yang, W. Synthesis of Large-Area Three-Dimensional Polyaniline Nanowire Networks Using a? Soft Template? *Macromol. Rapid Commun.* **2005**, *26*, 395−400.

(18) Li, G.; Li, Y.; Li, Y.; Peng, H.; Chen, K. Polyaniline Nanorings and Flat Hollow Capsules Synthesized by *in Situ* Sacrificial Oxidative Templates. *Macromolecules* **2011**, *44*, 9319−9323.

(19) Simotwo, S. K.; Delre, C.; Kalra, V. Supercapacitor Electrodes Based on High-Purity Electrospun Polyaniline and Polyaniline-Carbon Nanotube Nanofibers. *ACS Appl. Mater. Interfaces* **2016**, *8*, 21261−21269.

(20) Virji, S.; Huang, J.; Kaner, R. B.; Weiller, B. H. Polyaniline Nanofiber Gas Sensors: Examination of Response Mechanisms. *Nano Lett.* **2004**, *4*, 491−496.

(21) Wang, J.; Chan, S.; Carlson, R. R.; Luo, Y.; Ge, G.; Ries, R. S.; Heath, J. R.; Tseng, H. R. Electrochemically Fabricated Polyaniline Nanoframework Electrode Junctions That Function as Resistive Sensors. *Nano Lett.* **2004**, *4*, 1693−1697.
(22) Huang, J. Syntheses and Applications of Conducting Polymer Polyaniline Nanofibers. *Pure Appl. Chem.* **2006**, *78*, 15−27.
(23) Li, H.; Wang, J.; Chu, Q.; Wang, Z.; Zhang, F.; Wang, S. Theoretical and Experimental Specific Capacitance of Polyaniline in Sulfuric Acid. *J. Power Sources* **2009**, *190*, 578−586.
(24) Wang, Y.; Yang, X.; Qiu, L.; Li, D. Revisiting the Capacitance of Polyaniline by Using Graphene Hydrogel Films as a Substrate: The Importance of Nano-Architecturing. *Energy Environ. Sci.* **2013**, *6*, 477−481.
(25) Kuila, B. K.; Nandan, B.; Böhme, M.; Janke, A.; Stamm, M. Vertically Oriented Arrays of Polyaniline Nanorods and Their Super Electrochemical Properties. *Chem. Commun.* **2009**, *38*, 5749.
(26) Li, J.; Xie, H.; Li, Y.; Liu, J.; Li, Z. Electrochemical Properties of Graphene Nanosheets/Polyaniline Nanofibers Composites as Electrode for Supercapacitors. *J. Power Sources* **2011**, *196*, 10775−10781.
(27) Peng, C.; Hu, D.; Chen, G. Z. Theoretical Specific Capacitance Based on Charge Storage Mechanisms of Conducting Polymers: Comment on 'Vertically Oriented Arrays of Polyaniline Nanorods and Their Super Electrochemical Properties.'. *Chem. Commun.* **2011**, *47*, 4105.
(28) Yu, Q. Z.; Shi, M. M.; Deng, M.; Wang, M.; Chen, H. Z. Morphology and Conductivity of Polyaniline Sub-Micron Fibers Prepared by Electrospinning. *Mater. Sci. Eng. B* **2008**, *150*, 70−76.
(29) Kuo, C. C.; Lin, C. H.; Chen, W. C. Morphology and Photophysical Properties of Light-Emitting Electrospun Nanofibers Prepared from Poly(Fluorene) Derivative/PMMA Blends. *Macromolecules* **2007**, *40*, 6959−6966.
(30) Massoumi, B.; Davtalab, S.; Jaymand, M.; Entezami, A. A. AB2 Y-Shaped Miktoarm Star Conductive Polyaniline-Modified Poly(Ethylene Glycol) and Its Electrospun Nanofiber Blend with Poly(ε-Caprolactone). *RSC Adv.* **2015**, *5*, 36715−36726.
(31) Lee, S. H.; Yoon, J. W.; Suh, M. H. Continuous Nanofibers Manufactured by Electrospinning Technique. *Macromol. Res.* **2002**, *10*, 282−285.
(32) Peng, S.; Zhu, P.; Wu, Y.; Mhaisalkar, S. G.; Ramakrishna, S. Electrospun Conductive Polyaniline-Polylactic Acid Composite Nanofibers as Counter Electrodes for Rigid and Flexible Dye-Sensitized Solar Cells. *RSC Adv.* **2012**, *2*, 652−657.
(33) Pinto, N. J.; Johnson, A. T.; MacDiarmid, A. G.; Mueller, C. H.; Theofylaktos, N.; Robinson, D. C.; Miranda, F. A. Electrospun Polyaniline/Polyethylene Oxide Nanofiber Field-Effect Transistor. *Appl. Phys. Lett.* **2003**, *83*, 4244−4246.
(34) Zhang, Y.; Rutledge, G. C. Electrical Conductivity of Electrospun Polyaniline and Polyaniline-Blend Fibers and Mats. *Macromolecules* **2012**, *45*, 4238−4246.
(35) Angelopoulos, M.; Ray, A.; Macdiarmid, A. G.; Epstein, A. J. Polyaniline: Processability from Aqueous Solutions and Effect of Water Vapor on Conductivity. *Synth. Met.* **1987**, *21*, 21−30.
(36) Xia, Y.; Wiesinger, J. M.; MacDiarmid, A. G.; Epstein, A. J. Camphorsulfonic Acid Fully Doped Polyaniline Emeraldine Salt: Conformations in Different Solvents Studied by an Ultraviolet/Visible/ Near-Infrared Spectroscopic Method. *Chem. Mater.* **1995**, *7*, 443−445.
(37) Xia, Y.; Macdiarmid, A. G.; Epstein, A. J. Camphorsulfonic Acid Fully Doped Polyaniline Emeraldine Salt: In Situ Observation of Electronic and Conformational Changes Induced by Organic Vapors by an Ultraviolet/ Visible/Near-Infrared Spectroscopic Method. *Macromolecules* **1994**, *27*, 7212−7214.
(38) Cao, Y.; Qiu, J.; Smith, P. Effect of Solvents and Co-Solvents on the Processibility of Polyaniline: I. Solubility and Conductivity Studies. *Synth. Met.* **1995**, *69*, 187−190.
(39) MacDiarmid, A. G.; Epstein, A. J. The Concept of Secondary Doping as Applied to Polyaniline. *Synth. Met.* **1994**, *65*, 103−116.
(40) Cheng, F.; Tang, W.; Li, C.; Chen, J.; Liu, H.; Shen, P.; Dou, S. Conducting Poly(Aniline) Nanotubes and Nanofibers: Controlled Synthesis and Application in Lithium/Poly(Aniline) Rechargeable Batteries. *Chem. - Eur. J.* **2006**, *12*, 3082−3088.
(41) Zhang, L.; Wan, M. Self-Assembly of Polyaniline—From Nanotubes to Hollow Microspheres. *Adv. Funct. Mater.* **2003**, *13*, 815−820.
(42) Wang, Q.; Yao, Q.; Chang, J.; Chen, L. Enhanced Thermoelectric Properties of CNT/PANI Composite Nanofibers by Highly Orienting the Arrangement of Polymer Chains. *J. Mater. Chem.* **2012**, *22*, 17612−17618.
(43) Yao, Q.; Wang, Q.; Wang, L.; Wang, Y.; Sun, J.; Zeng, H.; Jin, Z.; Huang, X.; Chen, L. The Synergic Regulation of Conductivity and Seebeck Coefficient in Pure Polyaniline by Chemically Changing the Ordered Degree of Molecular Chains. *J. Mater. Chem. A* **2014**, *2*, 2634−2640.
(44) Ran, F.; Tan, Y.; Liu, J.; Zhao, L.; Kong, L.; Luo, Y.; Kang, L. Preparation of Hierarchical Polyaniline Nanotubes Based on Self-Assembly and Its Electrochemical Capacitance. *Polym. Adv. Technol.* **2012**, *23*, 1297−1301.
(45) Yan, J.; Wei, T.; Fan, Z.; Qian, W.; Zhang, M.; Shen, X.; Wei, F. Preparation of Graphene Nanosheet/Carbon Nanotube/Polyaniline Composite as Electrode Material for Supercapacitors. *J. Power Sources* **2010**, *195*, 3041−3045.
(46) Zhou, K.; He, Y.; Xu, Q.; Zhang, Q.; Zhou, A.; Lu, Z.; Yang, L. K.; Jiang, Y.; Ge, D.; Liu, X. Y.; et al. A Hydrogel of Ultrathin Pure Polyaniline Nanofibers: Oxidant-Templating Preparation and Supercapacitor Application. *ACS Nano* **2018**, *12*, 5888−5894.
(47) Frontera, P.; Busacca, C.; Trocino, S.; Antonucci, P.; Lo Faro, M.; Falletta, E.; Della Pina, C.; Rossi, M. Electrospinning of Polyaniline: Effect of Different Raw Sources. *J. Nanosci. Nanotechnol.* **2013**, *13*, 4744−4751.
(48) Chaudhari, S.; Sharma, Y.; Archana, P. S.; Jose, R.; Ramakrishna, S.; Mhaisalkar, S.; Srinivasan, M. Electrospun Polyaniline Nanofibers Web Electrodes for Supercapacitors. *J. Appl. Polym. Sci.* **2013**, *129*, 1660−1668.

https://dx.doi.org/10.1021/acsami.9b21696
ACS Appl. Mater. Interfaces 2020, 12, 19369−19376